PRECISE GPS/ACOUSTIC POSITIONING OF SEAFLOOR REFERENCE POINTS FOR TECTONIC STUDIES

Fred N. Spiess, C. David Chadwell, John A. Hildebrand

Marine Physical Laboratory, Scripps Institution of Oceanography, UCSD, San Diego, CA 92093

Larry E. Young, George H. Purcell, Jr.

Jet Propulsion Laboratory, California Institute of Technology, Pasadena, CA 91109

Herb Dragert

Geological Survey of Canada, Pacific Geoscience Centre, Sidney, BC, CANADA V8L 4B2

Abstract

Global networks for crustal strain measurement provide important constraints for studies of tectonic plate motion and deformation. To date, crustal strain measurements have been possible only in terrestrial settings: on continental plates and island sites within oceanic plates. We report the development of technology for horizontal crustal motion determination at seafloor sites, allowing oceanic plates to be monitored where islands are not available. Seafloor crustal monitoring is an important component of global strain measurement because about 70% of the Earth's surface is covered by water, and this region contains most of the tectonic plate boundaries and zones of crustal deformation.

Using the Global Positioning System (GPS) satellites and underwater acoustics, we have established a geodetic reference site on the Juan de Fuca plate at 2.6 km depth, approximately 150 km off the northwest coast of North America. We measure the baselines between this site and two terrestrial GPS stations on Vancouver Island, British Columbia. The Juan de Fuca plate site is an appropriate setting to develop seafloor observation methods, since it is a well studied

area, easily accessible from west coast Canadian and United States ports. Determination of seafloor motion at this site addresses questions related to convergence between the Juan de Fuca and North American plates across the Cascadia Subduction Zone.

At the Juan de Fuca seafloor geodetic reference site we installed precision acoustic transponders on the sea floor, and measured ranges to them from a sound source at a surface platform (ship or buoy). The platform is equipped with a set of three GPS antennas allowing determination of the sound source position at times of signal transmission and reception. Merging the satellite and acoustic data allows determination of the transponder network location in global reference frame coordinates. Data processing to date suggests repeatabilities of ± 0.8 cm north and ± 3.9 cm east in the seafloor transponder network position relative to reference points on Vancouver Island.

1. Introduction

With the advent of space-based geodesy — Very Long Baseline Interferometry (VLBI), Satellite Laser Ranging (SLR) and Global Positioning System (GPS) techniques — global networks have come into being for study of crustal dynamics (e.g. Noll, 1997). The primary goal of these networks is the understanding of plate motion and deformation. Since the above techniques all involve use of electromagnetic energy that does not penetrate significantly into sea water, there are large gaps in global coverage, just as there are gaps in global seismic and geomagnetic observation systems. Islands can fill these gaps to some extent, but there are large expanses of the ocean-covered 70% of the Earth without islands. In addition to some of the smaller plates (e.g. Juan de Fuca plate) that have no islands, there is the example of the Pacific plate — the largest of all the crustal tectonic elements — on which the only available mid-plate

reference points above 5°N are on the Hawaiian Islands.

The need for ocean floor reference points is particularly acute for understanding tectonic phenomena near plate boundaries, since most plates have at least one boundary in the oceanic realm. Unfortunately the nature of the phenomena being studied works against the availability of island stations. The new crust at normal ridge crests is too thin to support island edifices. At the other extreme, downwarping of old crust at most subducting margins submerges the islands as they approach the convergent boundary trenches.

This paper describes progress being made to fill these gaps in oceanic coverage for horizontal crustal motions. The first seafloor geodetic installation was made to provide data on the Juan de Fuca plate seaward of the Cascadia Subduction Zone (Fig. 1). This site is a particularly logical one because of its societal significance (seismic hazards), the wealth of previous seafloor mapping studies (e.g. Hyndman et al., 1990), and its logistic convenience for seagoing operations based on the west coast of Canada and the United States.

The possibility of creating geodetically relevant seafloor reference points, using GPS techniques linked to the sea floor by acoustic means, was first established in the mid-1980's. It was based on the independent developments of kinematic GPS positioning and of precision methods for measuring underwater sound travel times over paths several kilometers long (Spiess et al., 1980; Spiess et al., 1997). In themselves these techniques would have been insufficient without the ability to cope with the constantly changing sound speed structure in the near surface portion of the water column (Nat'l Res. Council, 1983). The key to solving this dilemma was visualized by Peter Bender (Nat'l Res. Council, 1981) and later brought to the attention of the sonar system developers (Spiess, 1985a). The essential element is recognizing that, to the extent that the oceanic sound speed structure is horizontally stratified, the location of the sea surface mid-point

above the center of a triangle of seafloor transponders is independent of the sound speed, being simply the point at which the three acoustic travel times to the transponders are equal.

This simple observation means that if one places transponders around an approximate circle on the sea floor, the circle center can be considered as a reference point, whose location can be recovered repeatedly with only approximate knowledge of the sound speed. From a central observation point, as the sound speed changes, the positions of the transponders will appear to move vertically in a coherent manner, but the horizontal center of the array will remain a well defined location.

The implementation of a real system embodying this concept involves a number of elements: a system concept, a kinematic GPS component, an underwater acoustic component, the application to a significant geophysical problem, and the necessary data reduction to deduce successive positions of the reference point relative to some appropriate terrestrial site. These elements will be described in the sections below.

2. CONCEPT

The GPS/Acoustic system concept is shown schematically in Fig. 2. The essence of this approach is to determine the acoustic ranges to the seafloor transponders from the sea surface point above the center of the transponder array, while simultaneously determining the location of the sea surface hydrophone with GPS. This requires a kinematic GPS component, an underwater acoustic component and a sea surface interface between these two components. The primary space-based GPS system provides the larger scheme on which this system is built, with the essential addition of recording data at one or more reference locations ashore at a data rate high enough to allow calculation of the shipboard antenna positions at least once per second.

The underwater component is based primarily on the use of precision acoustic transponders (Spiess et al., 1980; Spiess et al., 1997). These units measure two way acoustic travel times between the hydrophone and the transponders with a resolution of a few microseconds, corresponding to a few mm in range. Spacing of the transponders was chosen as a compromise between two competing factors. The sound speed differences between the several sea floor to sea surface paths will be smaller if the paths are closer to each other, arguing for small separations among the transponders. Consideration of the geometric strength, however, dictates use of the widest possible transponder spacings. The end result was selection of transponder locations on a circle with radius approximately equal to the water depth (Spiess, 1985a). The integrated water column sound speed is determined from measurements of temperature and salinity as a function of depth (Millero and Li, 1994; Chen and Millero, 1977; Del Grosso, 1974), or directly with a precision sound velocity meter at the observation times (Boegeman et al., 1990).

The interface between the GPS and the underwater acoustic system component is provided by a ship or buoy equipped with three GPS receivers and an underwater hydrophone, all connected by a rigid structure. In this situation, the positions of the three GPS units, and the geometry of the structure on which they and the hydrophone are mounted, provide the necessary information to calculate the hydrophone location at the times of signal transmission and reception. To make the necessary calculations, it is adequate to determine the GPS position of the hydrophone once per second. The acoustic transmit time can be synchronized with times of GPS position determination, and the hydrophone location at receive time can be interpolated between the once per second points.

The most desirable surface vehicle would be a tautly moored buoy; however, the deep water installation of such a platform is more time consuming than simply maintaining a ship at

the array center for the few days that we have had available on station. Therefore, we have favored using a maneuverable ship as the surface vehicle.

The shipboard installation uses a 1-m-diameter access tube extending from the upper deck of the ship through the bottom of the hull. A hydrophone is installed in the access tube bottom, backed with an optical corner reflector visible at the upper deck through a watertight viewing tube. The GPS antennas are mounted on tightly guyed extensions to the ship's masts, and each of the three GPS antennas is backed with an optical corner reflector. A range and angle measuring survey instrument is mounted above the hydrophone viewing tube to determine the relative positions of the four elements — the three antennas and the hydrophone. With these data, and auxiliary measurements of the individual antenna and hydrophone configurations, the location of the phase center of the hydrophone relative to the phase centers of the GPS antennas is measured with mm accuracy. The geodetic position of the hydrophone can thus be calculated from the GPS data at each transmit or receive time.

3. GPS COMPONENT

Decimeter-level hydrophone positioning is accomplished by determining the locations of the GPS antennas on the platform relative to one or more stations on shore. Our approach uses GPS L1 and L2 range and phase data at each of the antennas. To determine the relative position at one second intervals, shipboard GPS data are recorded at a one second rate from a set of three TurboRogue receivers, while shore stations record the data either directly at a one second rate, or with a data compression scheme such that once-per-second data can be retrieved.

Though similar to processing techniques used for terrestrial GPS crustal motion measurement (Feigl et al., 1993), the GPS/Acoustic approach accommodates the motion of the shipboard

antennas and capitalizes on the proximity of the shipboard GPS equipment by using a common frequency standard and zenith tropospheric delay model (Fig.3). The primary observable is the ionosphere-free double difference phase combination, formed between various antenna pairs on the ship and shore, with attempted carrier phase ambiguity resolution (Blewitt, 1989). Jet Propulsion Laboratory (JPL) orbits, estimated from data collected at a global network of tracking stations, are used as *a priori* information. Currently, the GPS data are processed in 4-hour segments to accommodate handling the once-per-second data.

The GPS/Acoustic platform position at one second intervals is determined relative to the shore station at Ucluelet on the west coast of Vancouver Island. If at least six satellites are visible, an hour of GPS data is sufficient to determine the platform coordinates in the frame of the global network with an uncertainty of ± 10 cm or better (Purcell et al., 1993).

4. UNDERWATER ACOUSTIC COMPONENT

The fundamental underwater acoustic elements are the precision transponders (Spiess et al., 1980; Spiess et al., 1997). These are a hybrid between conventional long baseline transponders (Boegeman, 1970) and echo repeaters. The transponders contain a precisely timed (± 1 μs) delay line that acts as buffer storage for incoming sound and is triggered by the conventional transponder recognition circuitry to play back the delay line contents. In this manner the timing portion of the transmitted signal travels through the water and the transponder delay line, ideally returning with its phase relationships to the original transmission undisturbed except for the travel time and buffer storage delays. A relatively broad band (quarter octave) timing signal is used, and the total time delay is determined by correlating the received signal with a stored replica of what was transmitted. The resulting time resolution for individual measurements can

be visualized from the shape of a correlogram made between our ship-mounted hydrophone and a precision transponder at a range of 7 km (Fig. 4). The location of the primary peak, and thus the round trip travel time, can easily be determined to within 5 μs, equivalent to about 4 mm in range. Sidelobes in the correlogram are due to the nature of the signal spectrum and transmission multipath structure, and they do not affect the timing accuracy obtained from the central correlation peak.

Once the transponders have been deployed on the sea floor, it is necessary to determine their relative positions. This is done by collecting acoustic range data using a vehicle towed a few hundred meters off the sea bottom. Near the sea floor, the sound speed field is relatively stable, and its values can be measured as the towed vehicle travels through its data collection path. The near-bottom acoustic technique (Spiess, 1985a; 1985b) collects simultaneous round-trip travel times (± 5 μs) from a hydrophone towed 200-400 m above the sea floor through the network, and measures the sound speed (± 10 ppm), and the depth of the hydrophone (± 10 cm), relative to the transponder depths. These observations are modeled with ray trace calculations through a multi-layered spherical ocean model (Horton, 1957; Biswas and Knopoff, 1970) and with distance calculations as geodesics on an ellipsoidal earth model (Vincenty, 1975). The differences between observation and model are inverted to determine, simultaneously, the centimeter-level relative positions of the towed hydrophone and the fixed transponders.

During the 1994 and 1995 visits to the array installed on the Juan de Fuca plate, near-bottom acoustic surveys were made. From these data we not only determined the relative geometry of the transponder array, but also evaluated the accuracy of the range-measuring system. After achieving the best adjustment of the array geometry, the residuals between the observed ranges and those calculated from the resulting array-position model place an upper

limit on the uncertainties inherent in the transponder/correlator system. The residual distribution, shown in the histogram of Fig. 5, has an RMS value of approximately 5 cm (Chadwell et al., 1996). The overall accuracy level of independent estimates of the relative transponder horizontal coordinates is ± 6 cm, based on 1994 and 1995 repeatability.

The sound speed versus depth profile has been determined from temperature and salinity data, using averaged values from many successive casts made during the time on station in each year for the continuously changing near surface structure. Given the lack of sound speed sensitivity of the transponder array center position, as discussed above, these approximations should not significantly alter the solutions for the array center location.

Combining the GPS and acoustic range data, and using the transponder array geometry derived from the near bottom surveys, we compute the differences between the observed and modeled ranges for each individual transponder. Inspection of the resulting GPS/Acoustic residual time series, given in Fig. 6, validates the assumption that the effects of the changing water column are coherent across the array. The residuals have a ± 5 cm scatter during any minute-long span of data. This scatter is comparable to that in the near bottom data given in Fig. 5. Over several minutes to hours, the residuals remain coherent, but exhibit trends with as much as 40 cm peak-to-peak variation. We attribute these short-term residual fluctuations to changes in the upper ocean sound speed structure which may be caused by internal waves and ocean tides. The upper 500 m of the ocean has a strong density gradient that is susceptible to internal wave oscillations, and hence sound speed variations over minutes-to-hours. Direct observation of sound speed changes that account for at most 20 cm of the peak-to-peak variations were made by simultaneous CTD profiling of the upper 300 m of ocean during GPS/Acoustic data collection.

A residual trend with a semi-diurnal period may be associated with ocean tidal effects,

though we cannot explain the mechanism that would result in 40 cm peak-to-peak variation. The direct effect of the surface platform rising and falling with the ocean tide is accommodated in the combined GPS and acoustic measurements of the total vertical offset between the shore station and the seafloor transponders. The vertical displacements due to the solid earth tide have been modeled in the GPS processing. The vertical displacements due to ocean loading have not been modeled, but this should result in less than 5 mm error in the relative horizontal positioning and less than 5 cm in vertical offset. In either the internal wave or ocean tide case, since the changes are coherent for all three transponders, there should be no horizontal shift in the array center location. As the upper ocean sound speed varies, the apparent acoustic ranges all increase or decrease together, which changes the vertical but not the horizontal coordinates of the array center.

5.CASCADIA SUBDUCTION ZONE RESULTS

In 1991, as one of the last program elements of the NASA Crustal Dynamics Program to initiate field work, and with seagoing support from the Canadian Pacific Geoscience Centre (PGC), our project made a trial seafloor transponder installation on the Juan de Fuca plate at 48°10′N, 127°10′W, 180 km west of the Juan de Fuca Strait (Fig. 1). Here it would be possible to make measurements to test models of the subduction process, thus providing a scientific context for the continued development of GPS/Acoustic geodesy.

The Juan de Fuca plate site was chosen to provide a first seaward observation point to complement the ongoing intensive terrestrial investigations of convergence across the Cascadia Subduction Zone and related deformation occurring between the northwest coast of North America and the interior of the North American plate (Hyndman et al., 1990; Dragert et al., 1994; Hynd-

man and Wang, 1995). The goal was to establish the present day motion of the Juan de Fuca plate relative to Vancouver Island. The specific site was selected on the basis of seismic reflection profiles (Davis and Hyndman, 1989) to lie beyond any appreciable deformation associated with continental margin tectonic processes in that area. Choice of the Juan de Fuca plate was particularly significant since there are no islands available to support any subaerial measurement capability for determining its motion, and its convergence with the North American plate is a potential source of seismic activity in the Pacific Northwest (Hyndman and Wang, 1995).

An array of four precision transponders was installed on the Juan de Fuca plate in 1991, using the C. S. S. John P. Tully, a Canadian research ship. Upon revisiting the site in 1993 with R/V Melville it was determined that some of the initially installed units were not providing adequate acoustic outputs to be useful in the long term, and two additional transponders were added to the original group. The array was further augmented by one transponder in 1994 and one further addition in 1995. Data processing has concentrated on the 1994, 1995 and 1996 surveys, using one of the 1991 transponders and the two from the 1993 installation. Throughout all of the observation epochs, shore stations on Vancouver Island, at Ucluelet and Sidney, have been maintained as the reference sites. In 1994, data were recorded at a one second interval at both locations. In 1995 and 1996, a special format was used to reduce the data recording requirements. In this format, a full suite of data was recorded every 30 seconds, and combined with a record of essential partial information from the once per second observations to allow reconstruction of an adequate equivalent of a 1 sec sample data set.

At this time all data from 1994, 1995 and 1996 have been reduced for the three transponders that were installed prior to 1994. This gives 1760 data points over a period of 23.6 hours for 1994, 17,913 during 32.0 hours for 1995, and 11,893 during 33.5 hours for 1996. The

data were processed in approximately four hour segments. Averaging the data over these segments reduces the effect of short term variations in the residuals (Fig. 6). Average position values for the array center for these four-hour blocks have been treated as individual measurements for purposes of this discussion.

From these individual 4-hour position measurements the average velocity from '94 to '96 of the seafloor array relative to Ucluelet is estimated, and the overall standard deviation of a GPS/Acoustic site visit position is assessed, in lieu of propagating the formal standard deviations through the GPS and acoustic data reduction algorithms. First, any motion during the two year span of these measurements is assumed to be linear and the position during any one site visit is taken to be the mean of all the individual 4-hour estimates collected during that visit. Also, for each site visit the GPS/Acoustic position standard deviation is assumed to be composed of a short term component, with characteristic periods less than 48 hours, the time on station for the survey, and a long term component that would not be averaged out during the site visit (Davis et al., 1989). Finally, the inverses of the sum of squared short-term and long-term errors, are used to weight the site visit mean position estimates in a linear fit to the three epochs.

The short term component may result from oceanographic effects, GPS and acoustic multipath and short period deflections of the antenna mounting structure. It is reflected in the scatter of the 4-hour position estimates relative to the site visit mean position. The sample standard deviation of the mean is adopted to be the short term component. For the '94, '95 and '96 data its values are $\pm$ 1.8 cm, $\pm$1.3 cm, and $\pm$ 0.8 cm, respectively, for the north component, and $\pm$ 1.7 cm, $\pm$ 1.5 cm, and $\pm$ 0.8 cm, respectively, for the east component. The progressively smaller values indicate improved precision with each site visit due to operational improvements that include maintaining the ship nearer the array center and increasing the time on station. The long

term components may result from oceanographic effects, GPS orbit error, and regional troposphere effects which tend to be correlated over several days (King et al., 1995). The long term component is reflected in the scatter of the mean position estimates about the linear fit. To obtain the long term component additional uncertainty is added until the linear fit weighted-residual-sum-of-squares divided by the degrees of freedom ($\hat{\sigma}_o^2$) is equal to one.

The linear fits are shown as solid lines in Fig. 7, and reveal a northeasterly trend for the motion of the Juan de Fuca plate site relative to southern Vancouver Island with components of 4.0 ± 0.9 cm/yr (1-σ) north and 1.1 ± 2.6 cm/yr (1-σ) east. For the north component $\hat{\sigma}_o^2$, is approximately equal to 1, thus no long term component was added to the annual estimated position uncertainties. For the east component an initial linear fit was performed weighting the mean positions only by the standard deviations of the mean, the short-term error component. The $\hat{\sigma}_o^2 = 8.2$ indicates that long term error components are also present. A long-term component of ± 3.8 cm was thus added to each short-term component to obtain $\hat{\sigma}_o^2 = 1$, and the linear fit was recalculated with the new weighting factors. These two-component standard deviations make the 1-σ GPS/Acoustic east position error as ± 4.2 cm, ± 4.1 cm and ± 3.9 cm in '94 to '96, respectively. These long term errors in the east component may be due to a known weakness in resolving the east GPS baseline component that is attributed to the characteristic orbital motion of GPS satellites (Bevis et al., 1995). Two remedies have been implemented by the crustal dynamics community; increase the the length of the survey and attempt to resolve the GPS phase ambiguities (Bock et al., 1993). GPS phase ambiguity resolution is being pursued with the existing data sets.

The GPS/Acoustic measurements for Juan de Fuca plate motion can be compared to expected velocities for the Juan de Fuca plate in the NUVEL-1A plate model (DeMets et al.,

1994), which are based on the magnetic anomaly trends from Wilson (1993). NUVEL-1A predicts the relative motion between the Juan de Fuca plate site and Ucluelet on Vancouver Island to be 2.1 cm northward and 3.8 cm eastward per year. Continuous terrestrial GPS measurements show Ucluelet is moving at 0.35 cm/yr ± 0.06 cm/yr (1-σ) northward and 0.79 cm/yr ± 0.13 cm/yr (1-σ) eastward relative to Penticton in the North American plate interior (Dragert, personal communication). This measured deformation of the North American plate boundary at Ucluelet, when subtracted from the NUVEL-1A rigid plate model prediction (dashed line in Fig. 7.) permits a comparison between measured GPS/Acoustic motion and expected motion for the Juan de Fuca plate. The GPS/Acoustic data suggest convergence between the Juan de Fuca plate seafloor site and North America, although with a greater northerly component than that given by the NUVEL-1A model. Due to the larger uncertainty in the GPS/Acoustic east-west motion estimate, both no convergence and convergence at the rate predicted by the plate model, could be consistent with the measured data.

6. CONCLUSIONS

The hardware, operational approaches and data analysis methods for seafloor geodesy are young in comparison with the decades of development for terrestrial applications of space-geodesy. However, the new technique we demonstrate in this paper should provide the essential oceanic coverage for determination of horizontal crustal deformation at seafloor sites. Developments to-date have allowed seafloor techniques to reach the stage of being useful, particularly in investigations of convergent plate boundaries. The Cascadia Subduction Zone results appear to validate the primary assumptions on which this approach is based. First, the near bottom measurements indicate that the underwater methods themselves can achieve individual measurement accuracies in the ± 5 cm range (Fig. 5). Second, they support the concept that, although there

may be substantial variations in upper ocean sound speed, these will largely be coherent over the short distances separating the acoustic paths to the transponders (Fig. 6) and thus have minimal effect on repeated determinations of the array center.

To provide perspective on the development of new geodetic positioning techniques, note the levels of accuracy, and the manner of improvement over the years, of VLBI (VLBI Group, 1995) and SLR (Belmont Workshop, 1995). Recent summary reports have illustrated this improvement (Fig. 8) and support the concept that further reductions in the uncertainties in seafloor reference point GPS/Acoustic methods will take place over the coming years.

Two aspects of the GPS/Acoustic approach seem likely to improve overall system performance. First is the use of moored buoys rather than ships for data collection. This will permit generation of much longer observation periods without the costs of maintaining ships on station. The improvements provided by continuous observations are well recognized in the terrestrial use of GPS (Bock et al., 1993). Integration of geodetic observation with other long term observing systems, particularly those in which buoys are maintained on station for climate or physical oceanographic research as in the Tropical Ocean-Global Atmosphere Program Tropical Atmosphere Ocean Array (TOGA-TAO), should make these long term observations cost-effective. Installation at sites of long term seismic or geomagnetic seafloor observatories with cable connections to shore would provide the modest amounts of power (2-3 watts) required to maintain the transponders in continuous operation indefinitely.

Second, in tectonically active areas, particularly near ridge crests, care must be taken to monitor complementary aspects of crustal deformation — local horizontal deformation and differential elevation change across the array. Because of the wide spacing between the seafloor transponders, any differential changes of elevation would give rise to displacement of the array

center reference point at the sea surface, and thus produce an apparent seafloor displacement, which could be misinterpreted as horizontal crustal motion. Similarly, changes in the transponder array internal geometry will change the location of the array center, and must be considered when interpreting the GPS/Acoustic data. For these reasons, near-ridge-crest installations should be made in collaboration with complementary programs to make near-bottom measurements of local strain and vertical displacement (Spiess and Hildebrand, 1995).

Finally, the results to date (Fig. 7) imply convergence across the Cascadia Subduction Zone. These initial results will be refined through further analyses of the data presently in hand, as well as through reoccupations in future years. In any event, these data are available for testing models of the convergence dynamics in this region.

Acknowledgements

Since the seagoing work to install and re-survey the transponder array at the Juan de Fuca plate/Cascadia Subduction Zone site was an essential element in our success, we are indebted to the scientists, technicians, and ship's crew members who provided the assistance necessary for conduct of successful operations. These include particularly Dr. C. J. Yorath, PGC Chief Scientist and John Anderson, captain of C. S. S. John P. Tully for the 1991 work; E. Buck, captain of R/V Melville in 1993, and R/V New Horizon captains Curt Johnson, John Manion and Robert Haines for operations in 1994, 1995, and 1996, respectively. In 1994, 1995 and 1996 shipboard GPS receivers were provided by the University NAVSTAR Consortium (UNAVCO). David Mencin of UNAVCO provided shipboard GPS support during the 1994 survey. Financial support for this program was provided by NASA and NSF.

References

Belmont Workshop Convenors, 1995. Satellite Laser Ranging Contributions to Earth Science: A synopsis of the 1994 Belmont SLR Workshop, Laboratory for Terrestrial Physics, Goddard Space Flight Center, Greenbelt MD 20771.

Bevis, M., Taylor, F. W., Schutz, B. E., Recy, J., Isacks, B. L., Helu, S., Singh, R., Kendrick, E., Stowell, J., Taylor, B., Calmant, S., 1995. Geodetic Observations of Very Rapid Convergence and Back-Arc Extension at the Tonga Arc, Nature, 374: 249-251.

Biswas, N. N., and L. Knopoff, 1970. Exact Earth-Flattening Calculation for Love Waves, Bull. Seismol. Soc. Am., 60, 4: 1123-1137.

Blewitt, G., 1989. Carrier Phase Ambiguity Resolution for the Global Positioning System Applied to Geodetic Baselines up to 2000 km. J. Geophys. Res., 94: 10187-10203.

Bock Y., Agnew, D. C., Fang, P., Genrich, J. F., Hager, B. H., Herring, T. A., Hudnut, K. W., King, R. W., Larsen, S. Minster, J-B., Stark, K., Wdowinski, S., and Wyatt, F. K., 1993. Detection of crustal deformation from the Landers earthquake sequence using continuous geodetic measurements. Nature, 361: 337-340.

Boegeman, D. E., 1970. High speed narrow band signal recognition circuit. U. S. Patent 3,517,214.

Boegeman, D. E., Lowenstein, C. D., and Spiess, F. N., 1990. Methods and system for measuring sound velocity. U. S. Patent No. 4,926,395.

Chadwell, C. D., Spiess, F. N., Hildebrand, J. A., Young, L. E., Purcell, G. H. Jr., and Dragert, H., 1997. Sea Floor Strain Measurement Using GPS and Acoustics. Proc. of GraGeoMar 96

Symposium; Univ. of Tokyo.

Chen, C. T., and Millero, F. J., 1977. Sound speed of seawater at high pressures. J. Acoust. Soc. Am., 62: 1129-1135.

Davis, E. E. and Hyndman, R. D., 1989. Accretion and recent deformation of sediments along the northern Cascadia subduction zone. Geol. Soc. Am. Bull., 101: 1465-1480.

Davis, J. L., Prescott, W. H., Svarc, J. L., and Wendt, K. J., 1989. Assessment of Global Positioning System Measurements for Studies of Crustal Deformation. J. Geophys. Res., 94: 13635-13650.

DeMets, C., Gordon, R. G., Argus, D. F., and Stein S., 1994. Effect of recent revisions to the geomagnetic reversal time scale on estimates of current plate motions. GRL v 21, no 20: 2191-2194.

Del Grosso, V. A., 1974. New equation for the speed of sound in natural waters (with comparison to other equations). J. Acoust. Soc. Am., 56: 1084-1091.

Dragert, H., Hyndman, R. D., Rogers, G. C., and Wang, K., 1994. Current deformation and the width of the seismogenic zone of the northern Cascadia subduction thrust. J. Geophys. Res., 99: 653-668.

Dragert, H., 1997. personal communication, Pacific Geoscience Centre, Sidney, CANADA.

Feigl, K. L., Agnew, D. C., Bock, Y., Dong, D., Donnellan, A., Hager, B. H., Herring, T. A., Jackson, D. D., Jordan, T. H., King, R. W., Larsen, S., Larson, K. M., Murray, M. H., Shen, Z., and Webb, F. H., 1993. Space Geodetic Measurement of Crustal Deformation in Central and

Southern California, 1984-1992. J. Geophys. Res., 98: 21677-21712.

Horton, J. W., 1957. The effects of the earth's curvature on sound ray paths in the sea, Res. Report No. 344, U.S Navy Underwater Sound Laboratory, New London, Conn.

Hyndman, R. D., Yorath, C. J., Clowes, R. M., and Davis, E. E., 1990. The northern Cascadia subduction zone at Vancouver Island: Seismic structure and tectonic history. Can. J. Earth Sci., 27: 313-329.

Hyndman, R. D., and Wang, K., 1995. The rupture zone of Cascadia great earthquakes from current deformation and the thermal regime. J.Geophys. Res. v 100, B11: pp. 22133-22154.

King, N. E., Svarc J. L., Fogleman, E. B., Gross, W. K., Clark, K. W., Hamilton, G. D., Stiffler, C. H., Sutton, J. M. 1995. Continuous GPS Observations Across the Hayward Fault, California, 1991-1994. J. Geophys. Res., 100: 20271-20283

Millero, F. J., and Li, X., 1994. Comments on "Equations for the speed of sound in seawater", 1993. [J. Acoust. Soc. Am.,: 93, 255-275.], J. Acoust. Soc. Am., 95: 2757-2759.

National Research Council Panel on Crustal Movement Measurements, 1981. Geodetic Monitoring of Tectonic Deformation - Toward a Strategy. pp. 43 & 44 and Rec. (c) page 5; National Academy Press, Washington D. C.

National Research Council Panel on Ocean Bottom Positioning (F. N. Spiess, Chair), 1983. Seafloor Referenced Positioning: Needs and Opportunities. NAS Press, Washington, DC, 53 pgs.

Noll, C. E., 1997. 1997 Bulletin. NASA Goddard Space Flight Center, Greenbelt, MD.

Purcell, G.H. jr., Young, L. E., Spiess, F. N., Boegeman, D. E., Lawhead, R. M. , Dragert, H., Schmidt, M., Jewsbury, G., Lisowski, M., and DeMets, D. C., 1993. Status of GPS/Acoustic Measurements of Seafloor Strain Accumulation across the Cascadia Subduction Zone. EOS, Trans. AGU, v. 74, no. 43: pg. 200.

Spiess, F. N., Boegeman, D. E., Pavlicek, F. V., and Lowenstein, C. D., 1980. Precision transponder and method of communication therewith. U. S. Patent 4,214,314.

Spiess, F. N., 1985a. Suboceanic geodetic measurements. IEEE Trans. on Geosciences and Remote Sensing; GE -23(4), pp 502-510.

Spiess, F. N., 1985b. Analysis of a possible seafloor strain measurement system. Marine Geodesy, 9: 385-398.

Spiess, F. N., and Hildebrand, J. A., 1995. Employing geodesy to study temporal variability at a mid-ocean ridge, EOS 76; 451,455.

Spiess, F. N., Boegeman, D. E., Zimmerman, R., Chadwell, C. D., and Hildebrand, J. A., 1997. Precision Transponder. SIO Ref. 97-3; Univ. of Calif., San Diego, Scripps Institution of Oceanography.

Vincenty, T., 1975. Direct and Inverse Solutions of Geodesics on the Ellipsoid with Application of Nested Equations, Survey Review, XXII, 176.

VLBI Group, 1995. VLBI - Measuring our changing earth. Brochure from Laboratory for Terrestrial Physics, Goddard Space Flight Center, Greenbelt MD 20771.

Wilson, D. S., 1993. Confidence Intervals for Motion and Deformation of the Juan de Fuca plate.

J.Geophys. Res., 98: 16,053-16,071.

FIGURE CAPTIONS

Fig. 1. The Juan de Fuca plate in the Northeast Pacific Ocean, showing the locations of the seafloor reference point (shaded dot) and the reference points on Vancouver Island (solid dot). Two baselines are shown spanning the Cascadia Subduction Zone trench.

Fig. 2. General configuration of the GPS/Acoustic approach to measuring the distance between a deep sea location and terrestrial reference points. GPS measurements are recorded at one second intervals at the three antennas on the ship or buoy and at the reference stations to calculate the location of the underwater acoustic hydrophone of the surface platform. At the same time, the hydrophone interrogates the seafloor precision transponders and receives their replies, measuring the round trip travel time, which is converted into distance using appropriate models for the underwater sound speed.

Fig. 3. Table showing the approach for reduction of the GPS data for seafloor geodesy. The satellite clocks are modeled as white noise parameters. The receiver clock at Ucluelet is adopted as a master clock. The receiver clock at Sidney is modeled as white noise. The three shipboard receivers are slaved to a common rubidium frequency standard. One receiver clock is modeled as white noise and the other two receiver clocks are modeled as constant offsets from the first receiver. The phase biases are modeled as constants. The zenith tropospheric delay is modeled as individual random walks at Ucluelet and at Sidney, and as a single random walk at the ship, common to all three shipboard antennas due to their proximity. The antenna coordinates at Ucluelet are tightly constrained, the antenna coordinates at Sidney are modeled as constants and the coordinates of each shipboard antenna are modeled as random walks. Jet Propulsion Laboratory orbits, estimated from data collected at a global network of tracking stations, are used as *a*

priori information.

Fig. 4. A correlogram between the stored transmitted signal and the signal received at a hull-mounted hydrophone from a precision transponder at a range of 7 km. Amplitude of the central peak is approximately 80% of that expected for perfect correlation. One centimeter resolution is clearly achievable in the timing resolution of the central peak.

Fig. 5. Histogram of acoustic slant range residuals from the 1995 near-bottom acoustic survey at the Juan de Fuca plate reference site. The RMS value is approximately 5 cm.

Fig. 6. Time series of GPS/Acoustic slant range residuals from the 1994 survey at the Juan de Fuca plate reference site for three transponders. The short term (minute) variations among the ranges are uncorrelated and comparable to the near bottom survey error distribution in Fig. 5. The long term (minutes-to-hours) variability is correlated among the three units, as expected for sound speed variations in the upper part of the water column. Since the long term variations are coherent for all three transponders, they do not shift the array center horizontal location.

Fig. 7. Apparent motion of the Juan de Fuca plate relative to Vancouver Island reference points measured using GPS/Acoustic techniques (squares), with error bars derived by comparing 4 hour subsets of the data with the mean for each site visit's data. The east component error bars also contain a long term component (see text for discussion). The solid line shows a linear fit, weighted by the position uncertainties, to the mean of 4 hour data segments for each site visit. The dashed line shows the slope expected from the NUVEL-1A global model minus the motion of the Island reference point relative to Penticton in the North American plate interior (DeMets et al., 1994; Dragert, personal commication).

Fig.8. Improvement of VLBI an SLR observational capabilities with time (VLBI Group, 1995; Belmont Workshop, 1994).

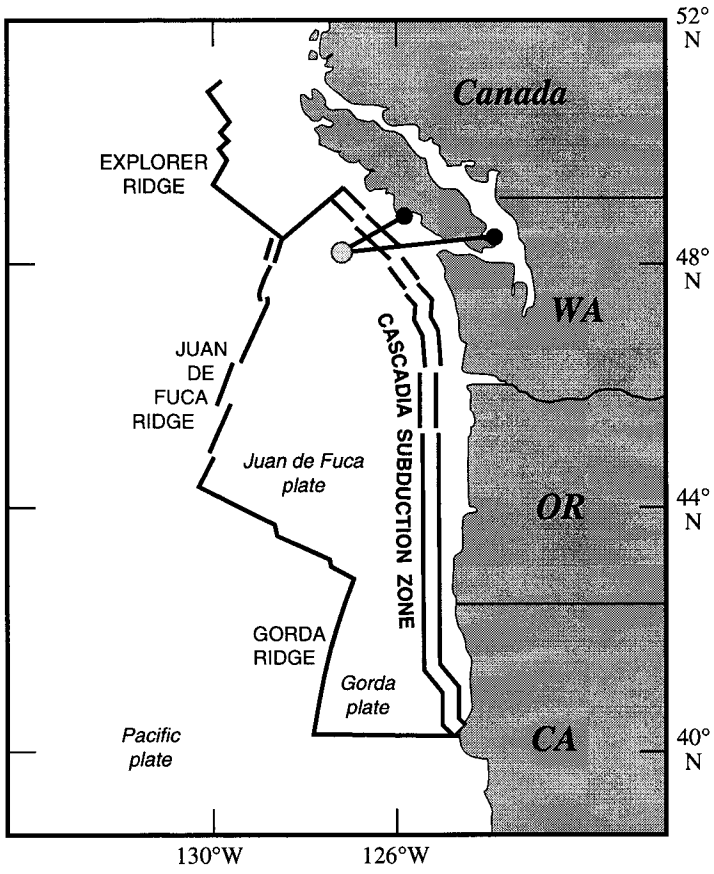
52°
N
Canada
EXPLORER
RIDGE
48°
N
WA
JUAN
DE
FUCA
RIDGE
CASCADIA SUBDUCTION ZONE
Juan de Fuca
plate
OR
44°
N
GORDA
RIDGE
Gorda
plate
Pacific
plate
CA
40°
N
130°W
126°W

FIG. 1

ESTIMATED PARAMETER	TYPE	NUMBER
Satellite Clock Offsets	Stochastic: white noise	≈ 6 x (# Epochs)
Station Clock Offsets (Sidney, Ship-1)	Stochastic: white noise	2 x (# Epochs)
Different'l Station Clock Offsets (Ship-2, Ship-3)	Constant	2
Phase Constants	Constant	≈ 60
Zenith Troposphere (Ucluelet, Sidney, Ship-1)	Stochastic: random walk (1 cm / $\sqrt{\text{hour}}$)	3 x (# Epochs)
Station Coordinates (Sidney)	Constant	3
Station Coordinates (Ship-1, Ship-2, Ship-3)	Stochastic: random walk (10 m / $\sqrt{\text{s}}$)	9 x (# Epochs)

FIG. 3

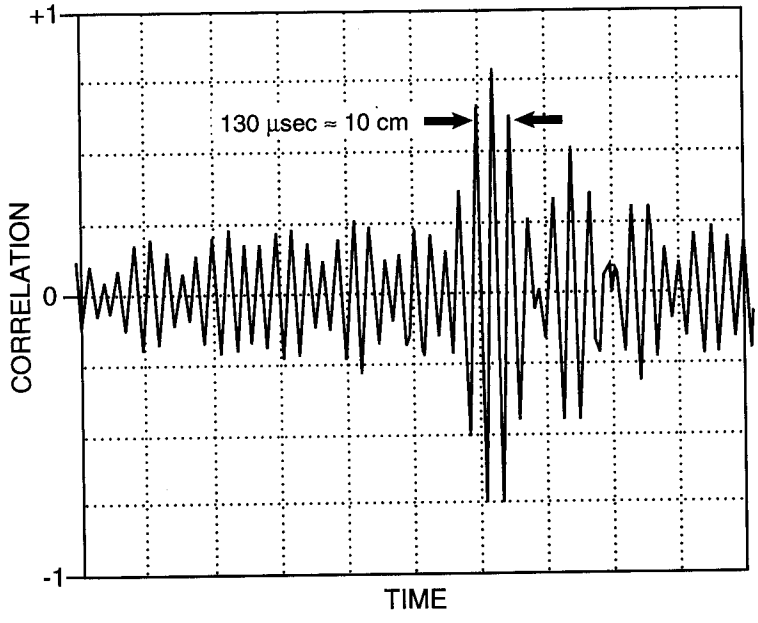

FIG. 4

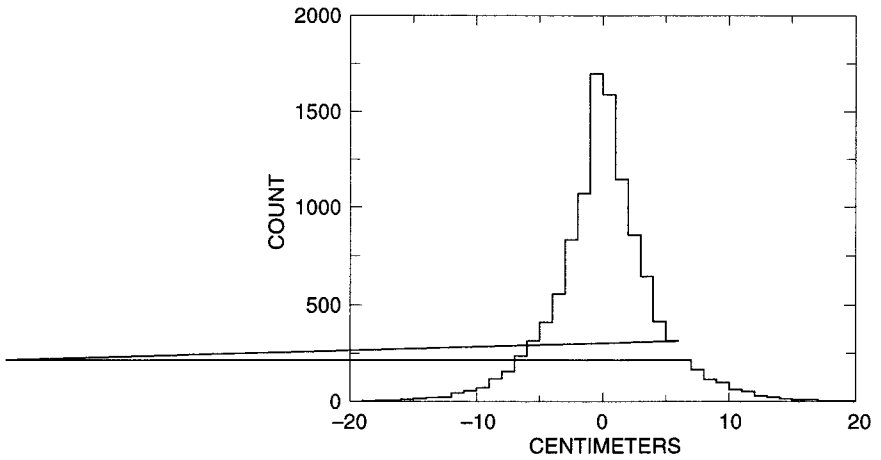

FIG. 5

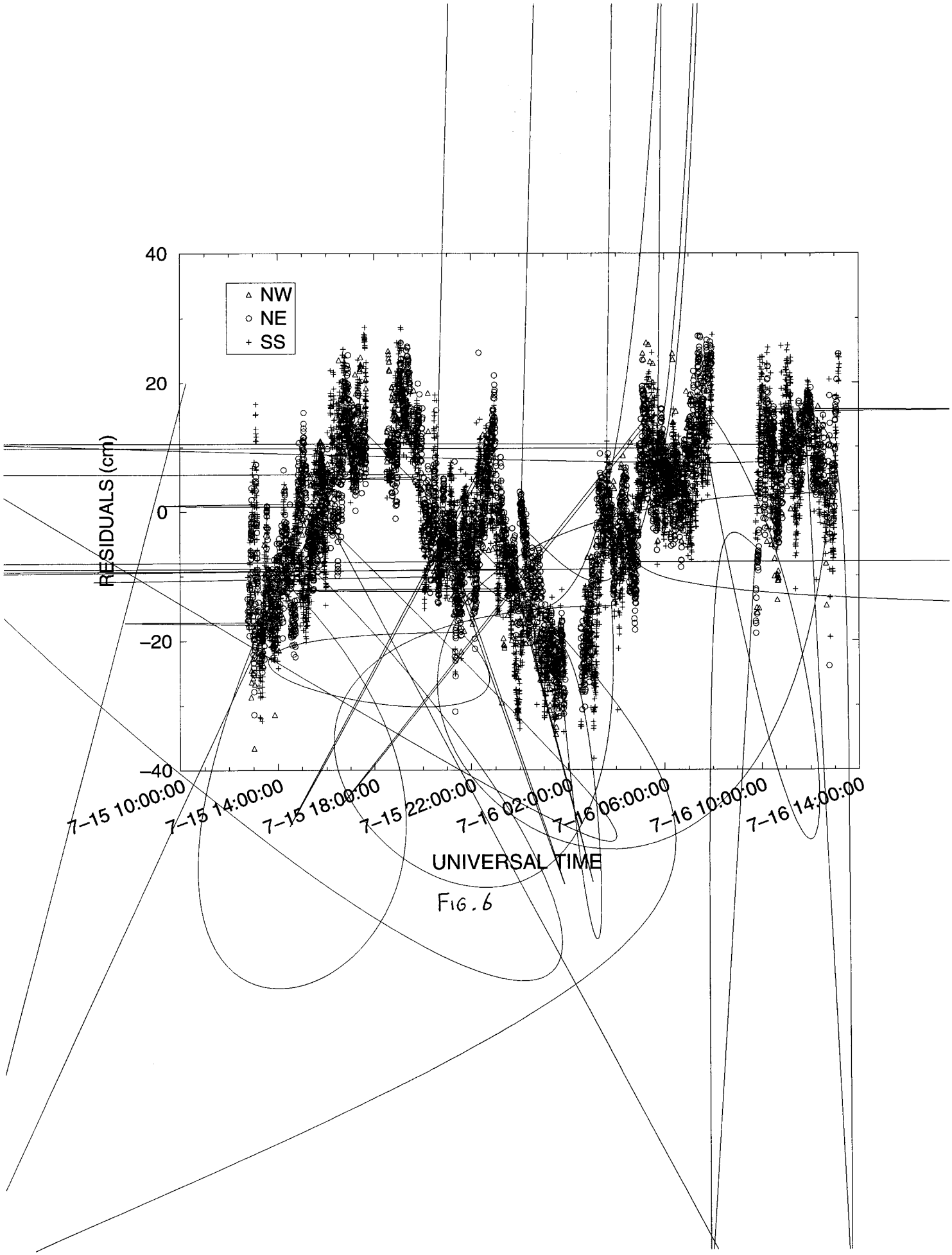
NW
NE
SS
40
20
0
−20
−40
RESIDUALS (cm)
7−15 10:00:00
7−15 14:00:00
7−15 18:00:00
7−15 22:00:00
7−16 02:00:00
7−16 06:00:00
7−16 10:00:00
7−16 14:00:00
UNIVERSAL TIME

FIG. 6

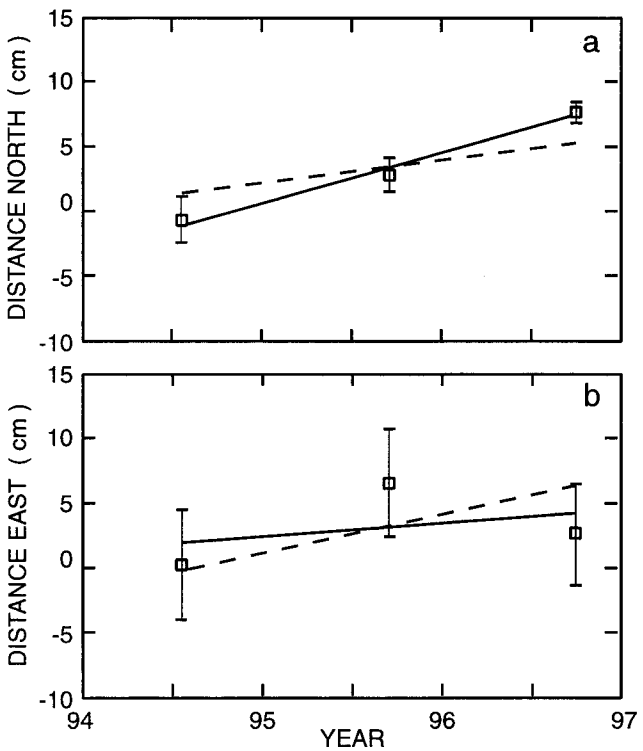
a
b
DISTANCE NORTH (cm)
DISTANCE EAST (cm)
15
10
5
0
-5
-10
94
95
96
97
YEAR

FIG. 7

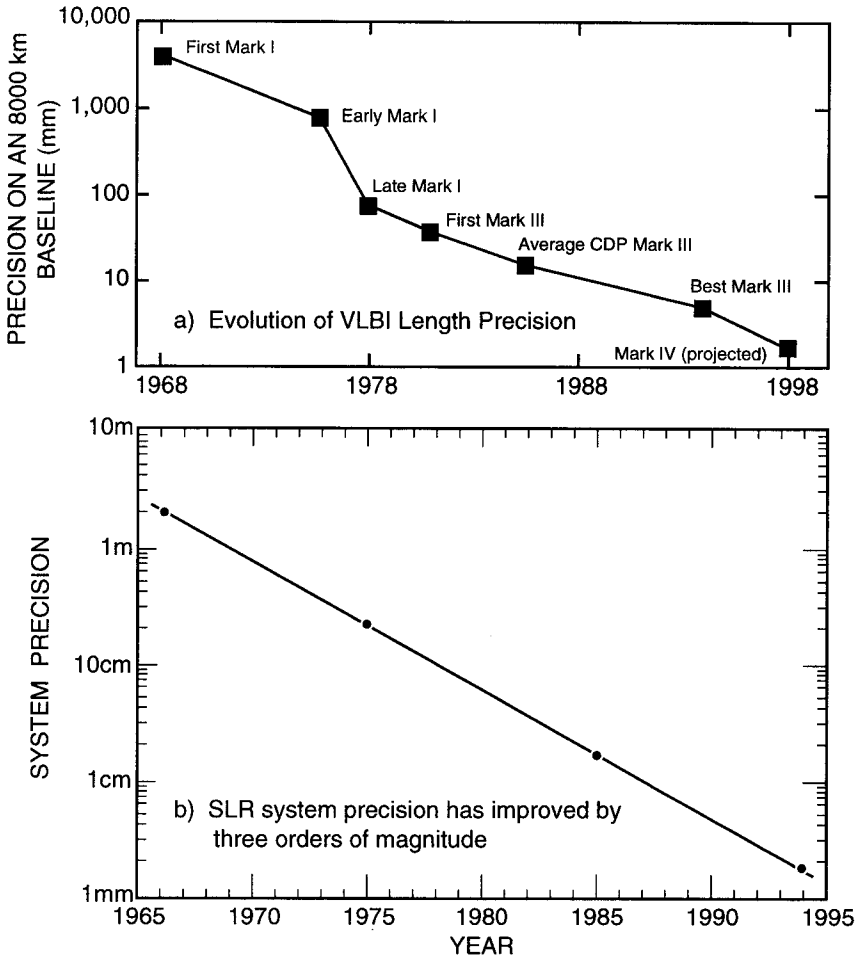
PRECISION ON AN 8000 km BASELINE (mm)
10,000
1,000
100
10
1
First Mark I
Early Mark I
Late Mark I
First Mark III
Average CDP Mark III
Best Mark III
Mark IV (projected)
a) Evolution of VLBI Length Precision
1968
1978
1988
1998
SYSTEM PRECISION
10m
1m
10cm
1cm
1mm
b) SLR system precision has improved by three orders of magnitude
1965
1970
1975
1980
1985
1990
1995
YEAR

Fig. 8

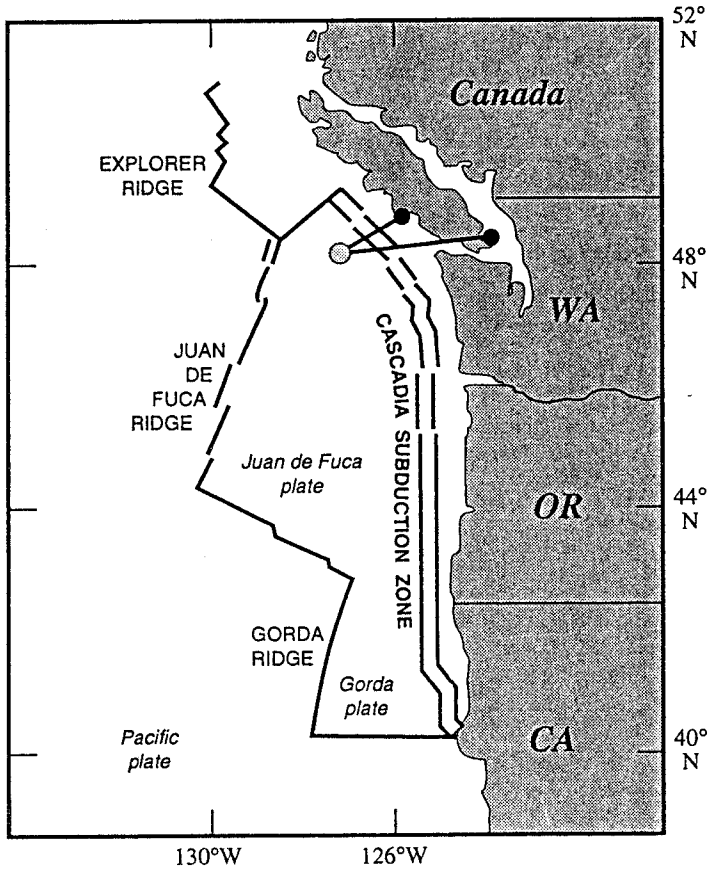

Figure 1
Spiess et al.

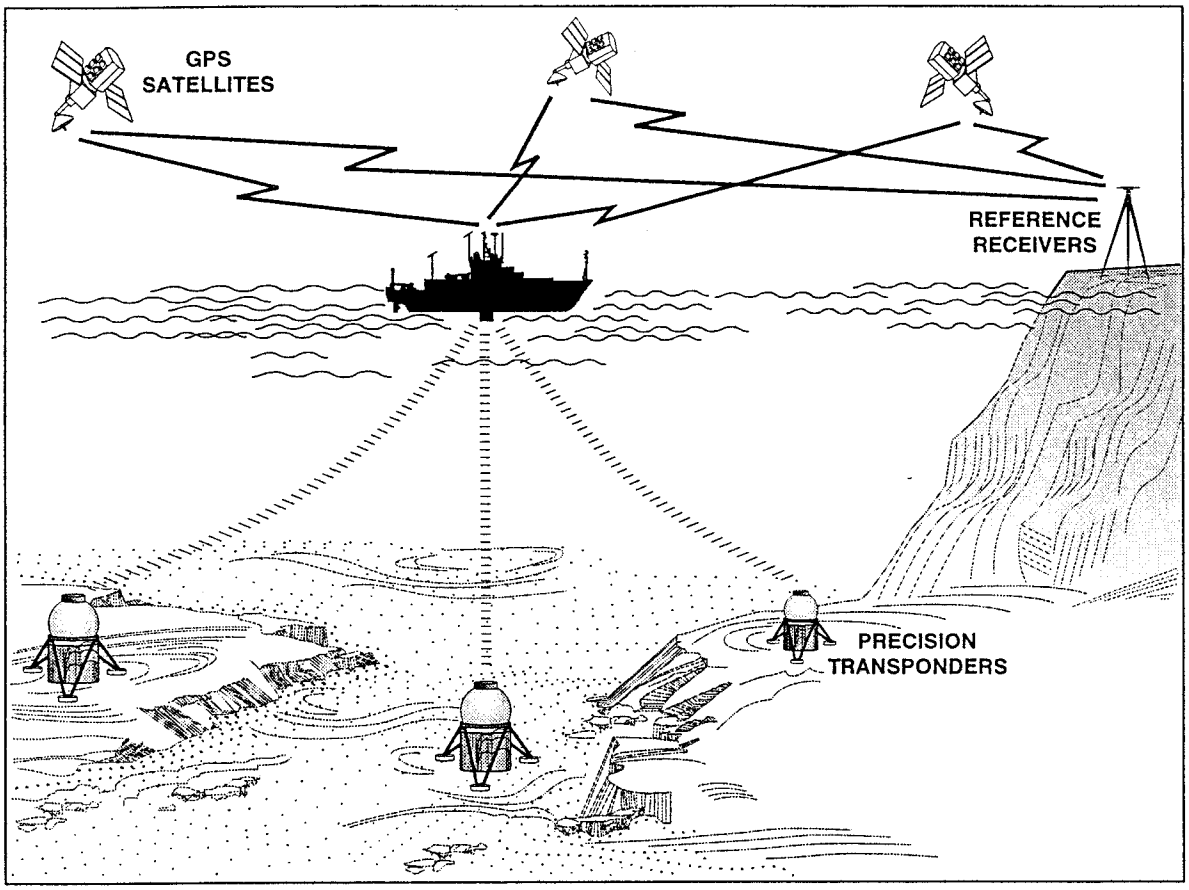

Figure 2
Spiess et al.

ESTIMATED PARAMETER	TYPE	NUMBER
Satellite Clock Offsets	Stochastic: white noise	≈ 5 x (# Epochs)
Station Clock Offsets (Sidney, Ship-1)	Stochastic: white noise	2 x (# Epochs)
Different'l Station Clock Offsets (Ship-2, Ship-3)	Constant	2
Phase Constants	Constant	≈ 60
Zenith Troposphere (Ucluelet, Sidney, Ship-1)	Stochastic: random walk (1 cm / $\sqrt{\text{hour}}$)	3 x (# Epochs)
Station Coordinates (Sidney)	Constant	3
Station Coordinates (Ship-1, Ship-2, Ship-3)	Stochastic: random walk (10 m / $\sqrt{\text{s}}$)	9 x (# Epochs)

Figure 3
Spiess et al.

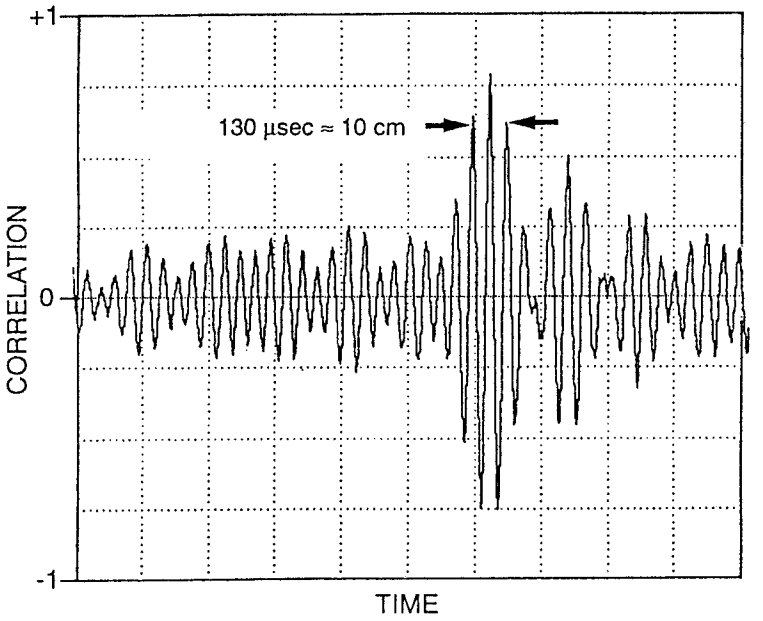

Figure 4
Spiess et al.

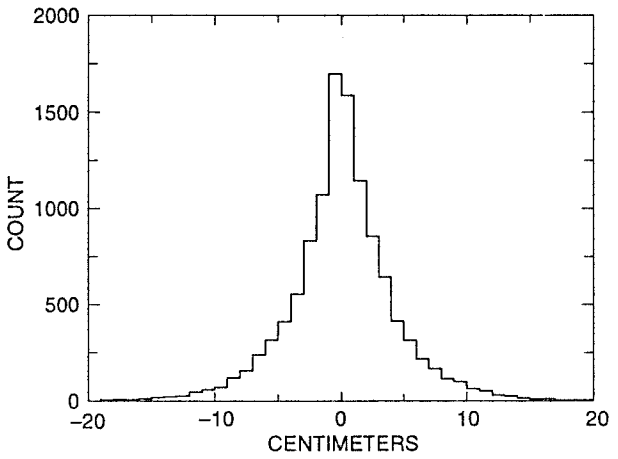

Figure 5
Spiess et al.

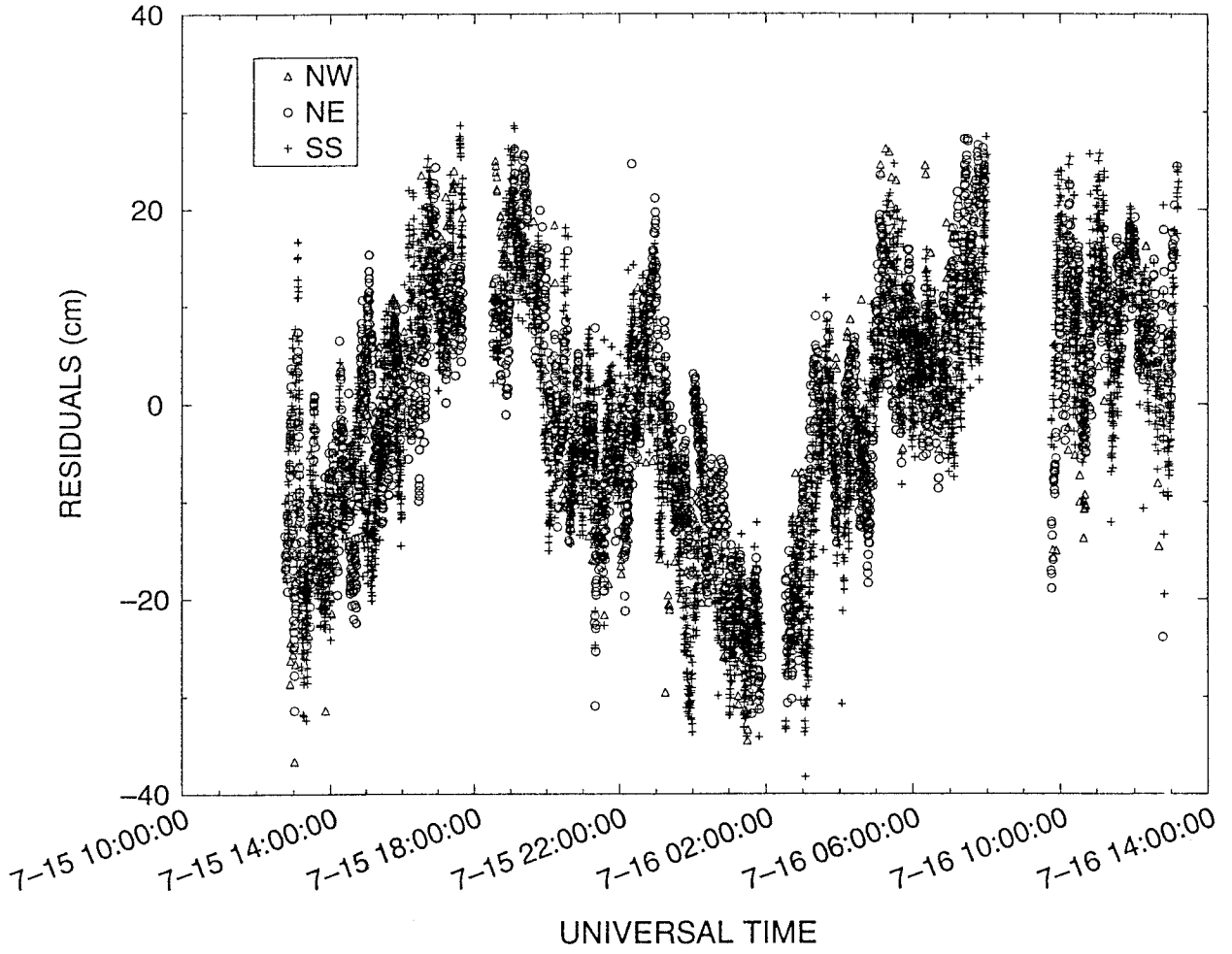

Figure 6
Spiess et al.

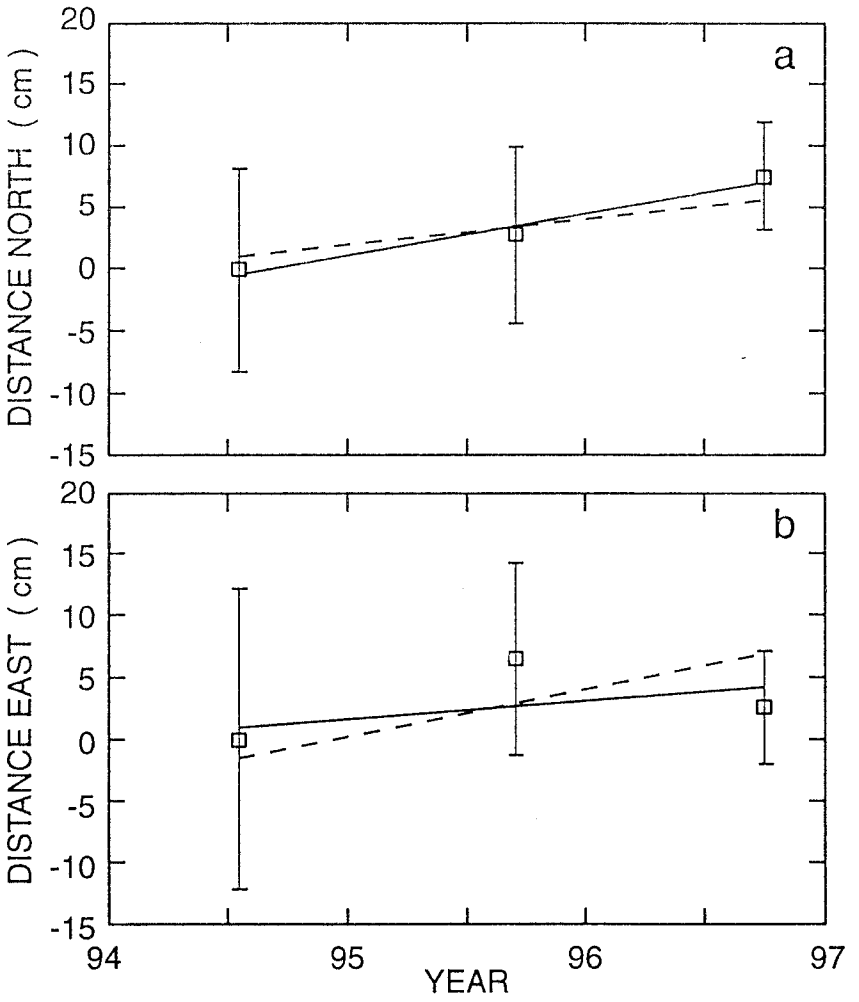

Figure 7
Spiess et al.

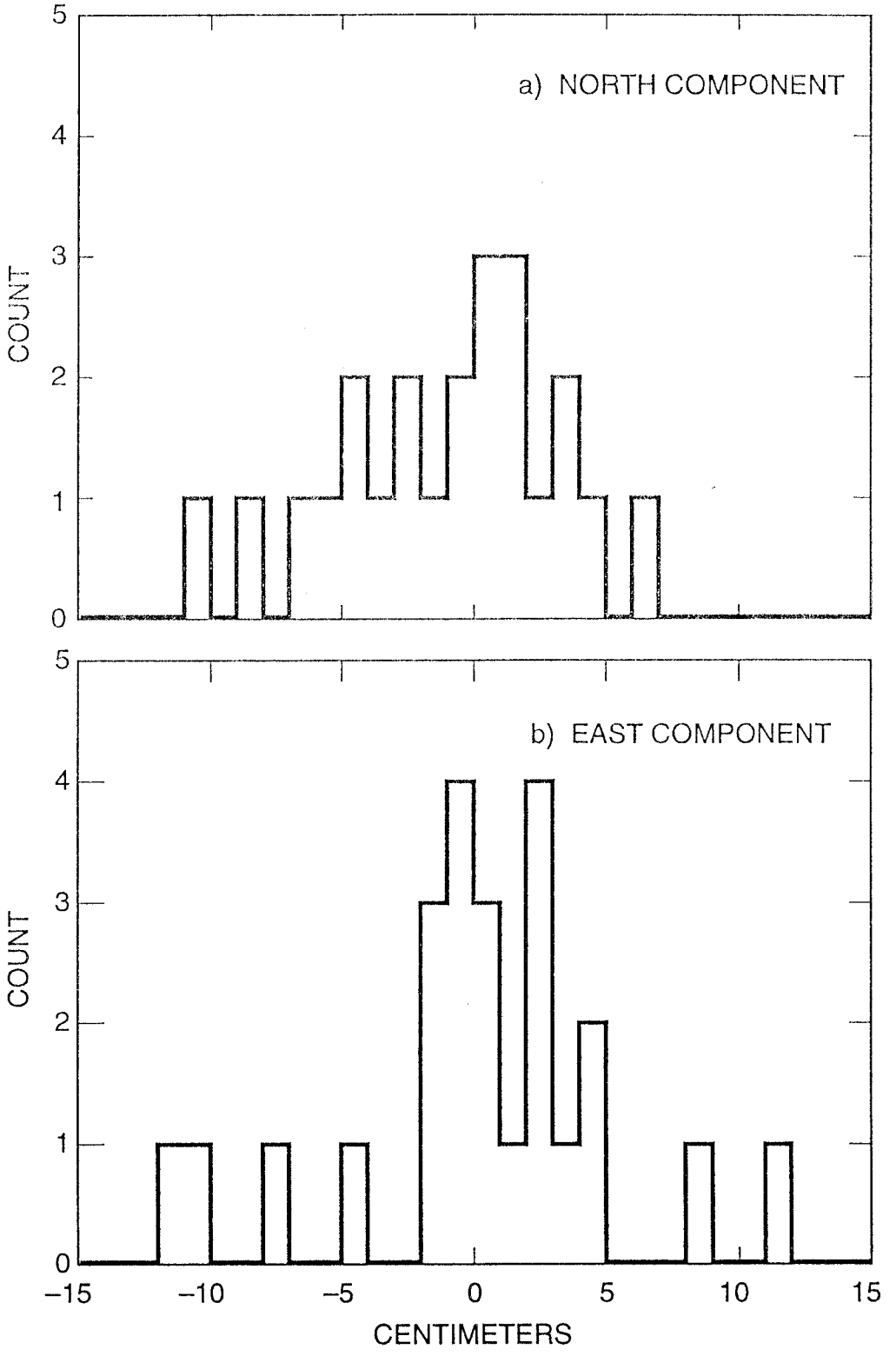

Figure 8
Spiess et al.

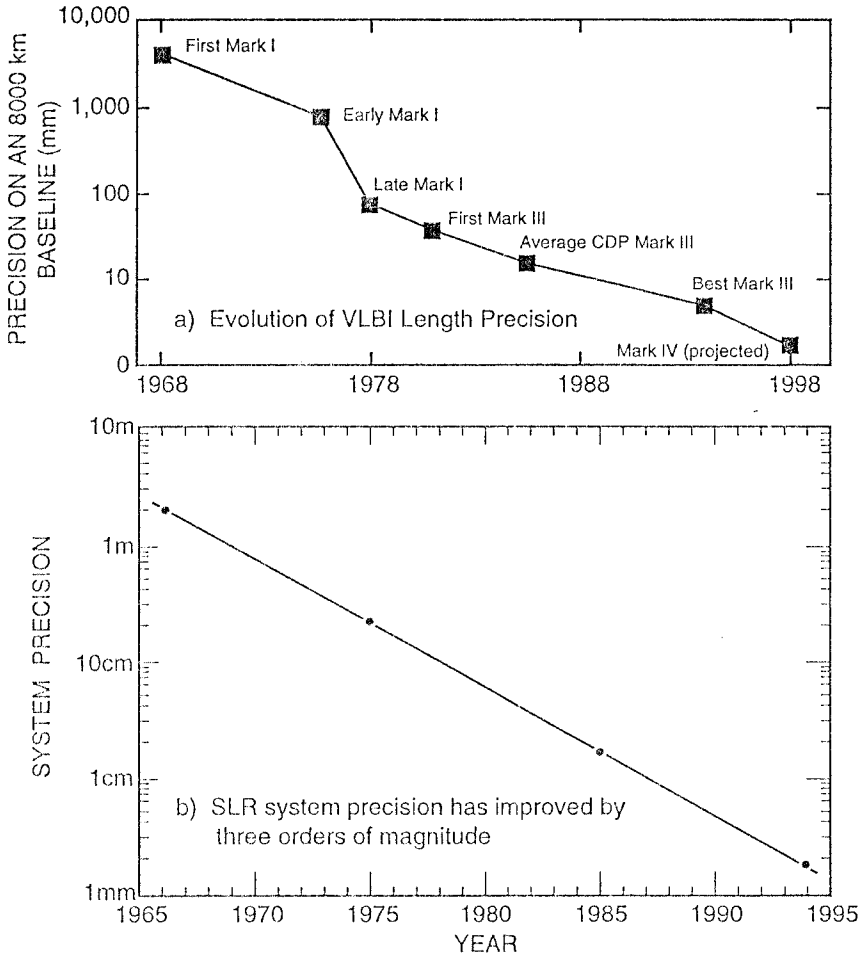

Figure 9
Spiess et al.